

Spectroscopic Investigation of the Gas-Phase Conformations of 15-Crown-5 Ether Complexes with K^+

Bruno Martínez-Haya,^{*,†} Paola Hurtado,[†] Ana R. Hortal,[†] Jeffrey D. Steill,[‡] Jos Oomens,[‡] and Patrick J. Merkling[†]

Departamento de Sistemas Físicos, Químicos y Naturales, Universidad Pablo de Olavide, 41013 Seville, Spain, and FOM Institute for Plasma Physics Rijnhuizen, Edisonbaan 14, NL-3439 MN Nieuwegein, The Netherlands

Received: March 10, 2009

Infrared multiple photon dissociation action spectra of the binary and ternary gas-phase complexes formed by 15-crown-5 ether with potassium cations ($15c5-K^+$ and $15c5-K^+-15c5$) are reported. The spectra span the 800–1500 cm^{-1} infrared range. Particularly significant differences are found in the position and structure of the CO-stretching band of the two types of complexes. The computational prediction at the DFT-B3LYP/6-31G* level of theory agrees well with the experimental observations, and provides a correlation between the spectral differences and the structural changes associated with the coordination of the ether oxygens with the alkali cation. The $15c5-K^+$ complex adopts a pyramidal structure, with the cation lying above the center of mass of the ether ring at a distance similar to its ionic radius. The ternary $15c5-K^+-15c5$ complex features a less tight coordination of the cation and a relative rotation between the backbones of the two crown ethers, which minimizes the intermolecular repulsions between the oxygens.

I. Introduction

The inclusion complexes formed by crown ethers with alkali metal cations constitute a textbook prototype of host/guest molecular recognition. They provide a relatively simple benchmark to elucidate the competition of intrinsic intermolecular interactions versus solvent effects leading to selective complex formation. For instance, in aqueous solution, the 18-crown-6 ether undergoes preferential complexation in the order $K^+ > Rb^+ > Cs^+ > Na^+ > Li^+$.^{1–3} For the 15-crown-5 ether, Na^+ and K^+ are preferred against the remaining alkali cations.⁴ These well-known properties are employed in separation and analytical applications. The selectivity of the crown-ether-alkali complexes is often interpreted in terms of the matching between the sizes of the metal cation and the cavity of the cyclic ether. Optimum size matching would provide the most favorable coordination between the cation and the oxygens of the ether. However, this apparently sensible argumentation does not hold for the gas-phase complexes, where the intrinsic ether-alkali coordination operates without interference from the solvent. Contrary to what is found in solution, the binding energies of the isolated (solvent-free) complexes formed by the 12-crown-4 (12c4), 15-crown-5 (15c5), and 18-crown-6 (18c6) ethers decrease monotonously with cation size; that is, it is in the order $Li^+ > Na^+ > K^+ > Rb^+ > Cs^+$.^{1–6} Qualitatively similar gas-phase affinities have been observed experimentally for linear polyethers.⁷

The disagreement between gas-phase affinities and expectations based on the size-matching model supports the key role played by solvation in the stabilization of the crown-ether-metal complexes in solution. In aqueous solution, the hydration of the alkali cation plays a crucial role, and it turns out that the exposure of the cation to the solvent in the ether complex enhances its stability.^{1,4} Cations smaller than the crown ether

cavity (e.g., $15c5-Li^+$ or $18c6-Na^+$) form inclusion complexes, with reduced access of the solvent. In contrast, larger cations form pyramidal-like structures, with the cation lying above the crown ether cavity. This latter configuration allows for a partial hydration of the complexed alkali cation. Therefore, the structure of the inclusion and pyramidal complexes in the gas phase can be used as an approximation to predict solution behavior as well as to calibrate *ab initio* methods. Also important, pyramidal structures are suitable for ternary complexes in which two crown ethers are bridged by the alkali cation. These sandwichlike complexes are the basis of selective molecular tweezers designed from crown ethers.⁸

Systematic experimental investigations of the complexes formed by the crown ethers with alkali metal cations were performed during the 1990s. These studies primarily focused on aggregation selectivity through the determination of relative binding energies. Armentrout and coworkers^{1,2} employed ion beam collision methods and found an enhancement in binding energy with decreasing cation size and growing crown ether size (e.g., ca. 3.1 eV for $18c6-Na^+$ and $15c5-Na^+$, 2.6 eV for $12c4-Na^+$, and 2.1 eV for $15c5-K^+$). These results were in qualitative agreement with the relative stabilities observed in early infrared multiple photon dissociation (IRMPD) experiments performed by Eyler and coworkers at a fixed wavelength (10.6 μm)⁵ and have been corroborated in more recent FT-ICR-MS experiments by Dearden and coworkers.⁶ Complementary to those studies, Bowers and coworkers explored the coarse-grain conformation of the crown-alkali complexes with ion mobility chromatography.^{8,9} They observed that each complex displays a single structure, with a cross section increasing with cation size as a consequence of a less-efficient inclusion of the metal inside the cavity.

A decade after the main body of the gas-phase experiments outlined above, spectroscopic measurements that address more directly the structure of the crown-ether-alkali inclusion complexes under isolated conditions are still lacking. This in contrast with the detailed theoretical studies reported since then

* Corresponding author. E-mail: bmarhay@upo.es.

[†] Universidad Pablo de Olavide.

[‡] FOM Institute for Plasma Physics Rijnhuizen.

TABLE 1: Structural Parameters Predicted by the DFT/B3LYP/6-31G* Theoretical Calculation for the Free 15c5 Crown Ether and for Its Complexes 15c5–K⁺ and 15c5–K⁺–15c5^a

	15c5	15c5–K ⁺	15c5–K ⁺ –15c5 (1)	15c5–K ⁺ –15c5 (2)
$d(\text{K}^+-\text{O})/\text{pm}$		272, 272, 269, 270, 274	297, 299, 285, 299, 318	295, 314, 297, 285, 300
$d(\text{O}_n-\text{O}_{n+1})/\text{pm}$	294, 293, 296, 300, 297	278, 287, 281, 277, 276	278, 290, 282, 279, 275	275, 279, 281, 290, 278
$\alpha(\text{O}_{n-1}\text{O}_n\text{O}_{n+1})$	117, 73, 158, 73, 117	116, 96, 106, 115, 93	122, 94, 104, 120, 88	122, 88, 120, 104, 94
$d(\text{K}^+-\text{c.o.m.})/\text{pm}$		156	210	208
$d(\text{K}^+-\text{c.o.m.}(\text{O}))/\text{pm}$		135	185	183
$d(\text{c.o.m.}-\text{c.o.m.}(\text{O}))/\text{pm}$	12	21	25	25
$E/(\text{kJ mol}^{-1})$	0	255	147	147
μ/D	1.69	1.08/2.30*	0.38/2.74*	0.38/2.74*

^a Parameters listed are illustrative of the spatial organization of the ether oxygen network that coordinates with the cation. In the case of the 15c5–K⁺–15c5 complex, one column is given for each of the crown ether moieties. Notation: d : distance; α : angle; c.o.m.: center of mass of the crown ether; c.o.m.(O): center of mass of the five oxygens in the same crown ether; E : binding energy of one ligand (eqs 1 and 2); μ : dipolar moment. (The asterisk denotes the partial dipole moment of the crown ether moiety, excluding the rest of the complex.)

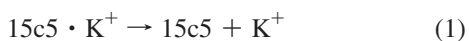
(e.g., see refs 4 and 10–13). Understanding the gas-phase conformations of the complexes is of importance to rationalize the key parameters that influence their molecular structure: cavity/cation size matching, charge density and polarizability of the cation, and flexibility of the ether backbone (which undergoes deformation upon complexation⁶).

We have undertaken a systematic investigation of the crown-ether–alkali systems, by means of mass-selected IRMPD action spectroscopy. We report here a study of the complexes formed by the 15c5 crown with K⁺. The results serve to illustrate the viability of the method to characterize the binary (15c5–K⁺) and ternary (15c5–K⁺–15c5) complexes from their rich IR spectra in the fingerprint region, including the CO stretches as major reference. Details of the experimental method are provided in Section II together with the theoretical approach used to compute the molecular structures. The results are then discussed and summarized in the subsequent Sections III and IV.

II. Methodology

A. Electrospray Ionization–Fourier Transform Ion Cyclotron Resonance Infrared Multiple Photon Dissociation Spectroscopy. Infrared multiple photon dissociation spectra were recorded using the Fourier transform ion cyclotron resonance (FTICR) mass spectrometer, described in detail elsewhere,¹⁴ coupled to the beamline of the free electron laser FELIX.^{15,16} The ionic complexes are produced by electrospray ionization (ESI) using a modified Waters Z-Spray source and solutions of 1 mM crown ether and KCl in a water/methanol mixture. Ions are accumulated in a hexapole ion trap and then pulse injected into the ICR cell, where they are mass isolated using a stored waveform inverse Fourier transform (SWIFT) excitation pulse. The mass-selected ions are then irradiated with typically 10 FELIX pulses, which are approximately 5 μs long and have a pulse energy of about 40 mJ. The spectral bandwidth of the radiation amounts to about 0.5% of the central wavelength. A further description of typical experimental procedures can be found in ref 17.

If the wavelength of FELIX is in resonance with a vibrational mode in the complex, then multiple photon absorption occurs, leading to dissociation of the parent ion. The observed fragmentation channels were



and

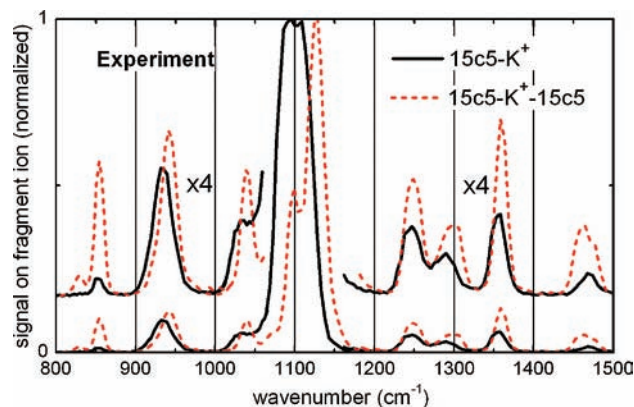


Figure 1. Experimental multiple photon infrared dissociation (ESI–FTICR IRMPD) spectra of the 15c5–K⁺ (solid line) and the 15c5–K⁺–15c5 (dashed line) crown-ether–potassium complexes. Each spectrum has been independently normalized so as to have a maximum intensity of unity. The most intense bands at ca. 935, 1000–1200, and 1360 cm^{−1} are mainly related to C–C stretching, C–O stretching, and CH₂ torsion vibrations, respectively.

For the latter process, weaker dissociation was also observed in the 15c5 + K⁺ + 15c5 channel, which was not included in the analysis. We constructed an IRMPD spectrum by plotting the relative ionic fragment yield as a function of the wavenumber of the radiation. The recorded spectra were linearly corrected for changes in laser pulse energy during the spectral scan.

B. Quantum Chemical Calculations. Quantum chemical calculations were performed at the DFT/B3LYP level of theory using a 6-31G* Gaussian basis set.¹⁸ Calculated IR frequencies are known to be overestimated and to require a correction factor of around 0.97 given the level of theory and basis sets employed.¹⁹ Therefore, all calculated frequencies indicated in this work in Figures and discussion were scaled by a factor 0.97, which consistently provided a good agreement with the experimental bands. The optimized structures are (at least) local minima because all frequencies are real. Where binding energies are indicated (Table 1), these have been obtained with correction for the vibrational zero point energies.

III. Results and Discussion

Figure 1 shows the ESI–FTICR IRMPD action spectra recorded for the 15c5–K⁺ and 15c5–K⁺–15c5 complexes in the 800–1500 cm^{−1} range. In this spectral region, optical absorption is basically related to C–O and C–C stretch vibrations, combined with C–O–C and C–C–O bending and torsion of the dihedral angles and of the CH₂ groups with respect to the cyclic ether backbone.¹⁰ The 1000–1200 cm^{−1} band,

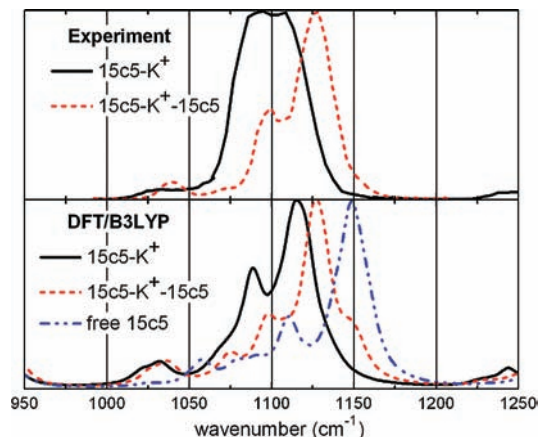


Figure 2. C–O stretching band of the experimental IRMPD spectra (top) of the $15c5-K^+$ (solid line) and the $15c5-K^+-15c5$ (dashed line) crown-ether–potassium complexes compared with the corresponding absorption spectra predicted by the DFT/B3LYP/6-31G* theory (bottom). The theoretical band predicted for the free 15c5 ether (dotted-dashed line) is also shown for reference. The theoretical spectra have been convoluted with the experimental broadening of 8 cm⁻¹. All spectra have been independently normalized so as to have a maximum intensity of unity.

associated essentially with C–O stretch vibrations, dominates the fragmentation yield in the IRMPD spectra. This band is expected to provide a sensitive probe of the oxygen–cation coordination. In fact, the spectra of the $15c5-K^+$ and the $15c5-K^+-15c5$ complexes present appreciable differences in the C–O stretching band. This is illustrated in greater detail in Figure 2, which shows that the C–O band of the ternary complex is more structured and overall displaced to higher wavenumbers.

Such significant changes observed in the C–O stretch vibrations of the two IRMPD spectra can be traced back to corresponding changes in the coordination of the oxygens with the K^+ cation in the two types of complexes. Figure 2 compares the two experimental action spectra with the IR absorption spectra predicted by the DFT computation in the 1000–1200 cm⁻¹ range. The theoretical spectrum for the isolated free crown ether is also shown for reference. The three DFT spectra were built from the vibrational transitions (after applying a single scaling factor of 0.97, see Section II) convoluted with a Gaussian broadening of 8 cm⁻¹. It can be observed that DFT predicts overall shifts of the $15c5-K^+$ and $15c5-K^+-15c5$ C–O stretch bands by ca. 35 and 20 cm⁻¹, respectively, with respect to the free 15c5 ether. Such prediction is in good agreement with the relative shift of the C–O bands in the two complexes observed experimentally. The greater shift for $15c5-K^+$ is related to tighter oxygen– K^+ interactions in comparison with $15c5-K^+-15c5$, as discussed below.

It can be observed that the DFT simulated spectra for the complexes display two main fairly resolved peaks at 1089 and 1115 cm⁻¹ for $15c5-K^+$ and at 1098 and 1127 cm⁻¹ for $15c5-K^+-15c5$. Whereas these two same peaks are present in the experimental spectra, they are only resolved in the case of the $15c5-K^+-15c5$ ternary complex. In the $15c5-K^+$ complex, the intensities of the two peaks become similar, and the two peaks almost coalesce and are barely appreciated as undulations on the flat top of the band. The greater experimental intensity of the 1089 cm⁻¹ band in the binary complex, in comparison with the 1098 cm⁻¹ band of the ternary one, is in fact well predicted qualitatively by the DFT calculation and can be explained from the more pronounced change in dipole

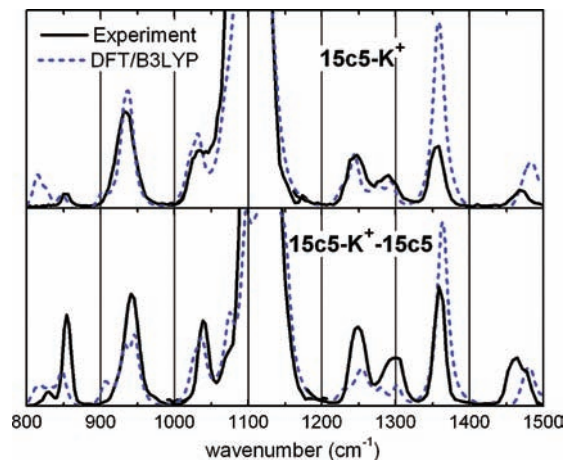


Figure 3. Full comparison of experimental IRMPD spectra (solid lines) of the $15c5-K^+$ (top) and the $15c5-K^+-15c5$ (bottom) complexes with the absorption spectra predicted by the DFT/B3LYP/6-31G* theory (dashed lines). The theoretical spectra have been convoluted with the experimental broadening of 8 cm⁻¹. The C–O stretching bands at 1000–1200 cm⁻¹, truncated in this representation, are shown in detail in Figure 2.

moment involved in the corresponding vibrational modes. The DFT analysis indicates that such modes predominantly involve the vibration of only one of the oxygens of the chain, which undergoes a symmetric C–O–C stretch and asymmetric O–C–C stretches. In the ternary complex, the same vibration occurs in each of the crown ethers, but the oxygens involved are opposite to each other, leading to a concerted vibration with a lesser overall change in the dipole moment.

Figure 3 compares in detail the full experimental IRMPD spectra (excluding the C–O band) with the prediction of the DFT computations. A sizable relative shift between the spectra of the two complexes is also observed for the peak at ~935 cm⁻¹, corresponding mainly to C–C stretching. For the remaining peaks, small shifts are also observed, although the major differences are more related to the relative intensities recorded. Excellent agreement is found for the position of the experimental bands, which indicates that the DFT vibrational frequencies obtained for the two types of complexes are accurate. Some discrepancy is observed for the relative intensities for the different bands across the spectrum, which may be attributed to the fact that experimental action spectra, involving multiple photon absorption, are being compared with DFT single photon absorption spectra.

The good overall agreement between experiment and DFT for the vibrational spectra of the two complexes lends support to the assignments and corresponding equilibrium molecular structures predicted by the theory. Such structures are described in Table 1 and represented graphically in Figure 4. To the best of our knowledge, the theoretical structure of the $15c5-K^+-15c5$ complex is reported here for the first time. The DFT results for the conformations of the free 15c5 ether and of the $15c5-K^+$ complex are in good agreement with the previous ab initio study of Hill and Feller at the MP2/6-31G* level.⁴ The present B3LYP/6-31G* $15c5-K^+$ binding energy of 255 kJ mol⁻¹ lies below the MP2/6-31G* value of 271 kJ mol⁻¹ reported in ref 4 but is still slightly above the 234 ± 13 kJ mol⁻¹ value determined in the ion–beam dissociation experiments of More and coworkers.¹

The structural parameters given in Table 1 are primarily intended to characterize the spatial organization of the ether oxygen network. Having an odd number of oxygens, the lowest

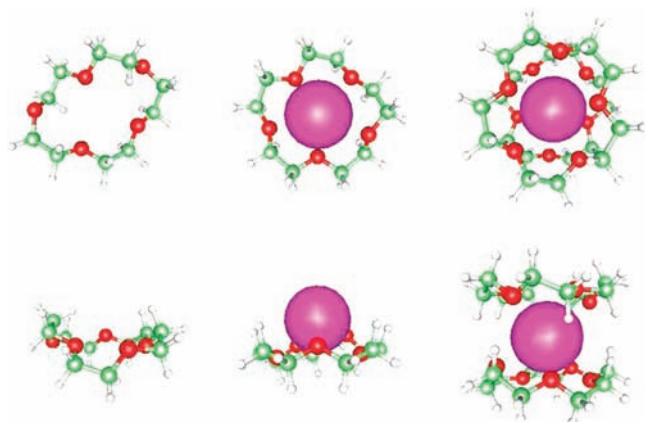


Figure 4. Graphical representation of the equilibrium geometry predicted by the DFT/B3LYP/6-31G* theoretical calculation for the free 15c5 crown ether (left) and for its complexes with the potassium cation, $15c5-K^+$ (middle) and $15c5-K^+-15c5$ (right). See Table 1 for quantitative information about some relevant structural parameters.

energy conformation of the free 15c5 already has an appreciable dipole moment (1.69 D). This is accompanied by a displacement of the center of mass of the oxygens with respect to the overall center of mass of the molecule (by 12 pm). It can be noticed that the elongated equilibrium conformation obtained for the free 15c5 ring in the present DFT calculation resembles that of conformer **1** of ref 4, which was almost isoenergetic with the lowest energy conformer in the MP2 calculation.

In the $15c5-K^+$ complex, the ionic radius of the K^+ cation (152 pm) is too large to fit into the crown cavity. (See Figure 4.) The cation places itself above the center of mass of the ether ring, at a distance of 156 pm, similar to its ionic radius. Nevertheless, a tight interaction with the cation takes place that induces significant changes in the structure of the crown ether with respect to the free 15c5. The complex adopts a distorted C_5 -like structure, with the oxygens oriented toward the cation to maximize the coordination energy. As a consequence, the 15c5 moiety has a greater dipole moment (2.30 D) than the free 15c5. In addition, the distance between the center of mass of the oxygens and the center of mass of the crown increases by almost a factor of two. (See Table 1.)

Similar considerations apply to the $15c5-K^+-15c5$ complex. In this case, however, the oxygen–cation coordination with each of the crown ethers is less tight. The distances between the K^+ cation and the oxygen atoms of the ether backbone are roughly 30 pm longer than those in the $15c5-K^+$ complex. Correspondingly, the distance between the cation and the center-of-mass of the crown ether moiety also increases by ca. 50 pm with respect to the $15c5-K^+$ complex. Nevertheless, the distortion of the crown ethers is still remarkable. It can be noticed that each of the 15c5 moieties acquires a net dipole moment of 2.74 D, even greater than in the $15c5-K^+$ complex. A noticeable difference with respect to the single crown complex is that in the ternary complex the repulsive interaction between the oxygens of the two crowns plays a relevant role. As can be appreciated in Figure 4, the $15c5-K^+-15c5$ complex features a relative rotation of $2\pi/10$ between the two crown ethers. In this way, the oxygens of the two ethers are intersected between each other, and the optimum coordination with the cation is combined with a minimization of the intermolecular repulsion between the lone-pair orbitals of the oxygens.

IV. Summary and Conclusions

The vibrational spectrum of the binary $15c5-K^+$ and ternary $15c5-K^+-15c5$ gas-phase complexes has been measured in the 800–1500 cm^{-1} range. Infrared multiple photon dissociation action spectroscopy has been applied for this purpose on ions prepared with the ESI–FTICR technique. Particularly pronounced differences are found in the structure of the CO–stretching band (1000–1200 cm^{-1}) of the two types of complexes. The computational prediction at the DFT–B3LYP/6-31G* level of theory corroborates that the spectral differences can be attributed to changes in the coordination of the oxygens of the ether backbone with the alkali cation. The good agreement between the experimental and the DFT results provides a consistent assignment of the vibrational spectra and of the corresponding conformations of the two complexes.

The oxygen–cation coordination is tighter and the attractive interactions are stronger in the $15c5-K^+$ complex than those in the sandwichlike $15c5-K^+-15c5$ complex. As a consequence, the CO stretching band is overall more shifted toward lower wavenumbers. The $15c5-K^+$ complex adopts a distorted C_5 structure in which the cation lies above the center of mass of the ether ring at a distance similar to its ionic radius. Within the ether, a collective displacement of the oxygens toward the cation takes place. As a consequence, the crown ether moiety significantly increases its dipole moment (2.30 D) with respect to the value of the free 15c5 (1.69 D).

In the pyramidal conformation of the $15c5-K^+$ complex, the cation is significantly exposed and can be partially solvated in solution. Partial hydration plays a determinant role in the selectivity of the complexation, which for the 15c5 crown ether favors Na^+ and K^+ against the other alkali cations.¹⁴ In addition, the exposure of the cation leads to the efficient formation of the ternary $15c5-K^+-15c5$ complex. Whereas this complex features a somewhat weaker coordination of the cation, an appreciable distortion of the crown ethers is still observed. Moreover, the repulsive interaction between the oxygens of the two crowns is minimized by means of a relative rotation between the crown ether backbones. This finding should be taken into account in the design of molecular tweezers based on crown ethers, which should provide enough flexibility to the ether groups so as to reach the more stable rotated configuration.⁸

Acknowledgment. The skillful assistance of Dr. B. Redlich and Dr. A. F. G. van der Meer as well as others of the FELIX staff is gratefully acknowledged. This work was supported by the European Community - Research Infrastructure Action under the FP6 “Structuring the European Research Area” Programme through the Integrated Infrastructure Initiative” Integrating Activity on Synchrotron and Free Electron Laser Science. We also acknowledge funding from the Regional Government of Andalucía (projects P06-FQM-01869 and P07-FQM-02600).

References and Notes

- (1) More, M. B.; Ray, D.; Armentrout, P. B. *J. Am. Chem. Soc.* **1999**, *121*, 417.
- (2) Armentrout, P. B. *Int. J. Mass Spectrom.* **1999**, *193*, 227.
- (3) Feller, D. *J. Phys. Chem. A* **1997**, *101*, 2723.
- (4) Hill, S. E.; Feller, D. *Int. J. Mass Spectrom.* **2000**, *201*, 41.
- (5) Peiris, D. M.; Yang, Y.; Ramanathan, R.; Williams, K. R.; Watson, C.; Eyster, J. R. *Int. J. Mass Spectrom. Ion Processes* **1996**, *157/158*, 365.
- (6) Anderson, J. D.; Paulsen, E. S.; Dearden, D. *Int. J. Mass Spectrom.* **2003**, *227*, 63.
- (7) Hortal, A. R.; Hurtado, P.; Martínez-Haya, B.; Arregui, A.; Banares, L. *J. Phys. Chem. B* **2008**, *112*, 8530.
- (8) Wyttenbach, T.; von Helden, G.; Bowers, M. T. *Int. J. Mass Spectrom. Ion Processes* **1997**, *165/166*, 377.

- (9) Lee, S.; Wyttenbach, T.; von Helden, G.; Bowers, M. T. *J. Am. Chem. Soc.* **1995**, *117*, 10159.
- (10) Al-Rusaese, S.; Al-Kahtani, A. A.; El-Ahzhary, A. A. *J. Phys. Chem. A* **2006**, *110*, 8676.
- (11) Glendenning, E. D.; Feller, D.; Thomson, M. A. *J. Am. Chem. Soc.* **1994**, *116*, 10657.
- (12) Kim, H. S. *J. Phys. Chem. B* **2004**, *108*, 11753.
- (13) Gajewski, M.; Tuszyński, J.; Mori, H.; Miyoshi, E.; Klobukowski, M. *Inorg. Chim. Acta* **2008**, *361*, 2166.
- (14) Valle, J. J.; Eyley, J. R.; Oomens, J.; Moore, D. T.; van der Meer, A. F. G.; von Helden, G.; Meijer, G.; Hendrickson, C. L.; Marshall, A. G.; Blakney, G. T. *Rev. Sci. Instrum.* **2005**, *76*, 023103.
- (15) Oepts, D.; van der Meer, A. F. G.; van Amersfoort, P. W. *Infrared Phys. Technol.* **1995**, *36*, 297.
- (16) FELIX. <http://www.rijnh.nl/felix/>.
- (17) Polfer, N. C.; Oomens, J. *Phys. Chem. Chem. Phys.* **2007**, *9*, 3804.
- (18) Frisch, M. J.; Trucks, G. W.; Schlegel, H. B.; Scuseria, G. E.; Robb, M. A.; Cheeseman, J. R.; Montgomery, J. A., Jr.; Vreven, T.; Kudin, K. N.; Burant, J. C.; Millam, J. M.; Iyengar, S. S.; Tomasi, J.; Barone, V.; Mennucci, B.; Cossi, M.; Scalmani, G.; Rega, N.; Petersson, G. A.; Nakatsuji, H.; Hada, M.; Ehara, M.; Toyota, K.; Fukuda, R.; Hasegawa, J.; Ishida, M.; Nakajima, T.; Honda, Y.; Kitao, O.; Nakai, H.; Klene, M.; Li, X.; Knox, J. E.; Hratchian, H. P.; Cross, J. B.; Bakken, V.; Adamo, C.; Jaramillo, J.; Gomperts, R.; Stratmann, R. E.; Yazyev, O.; Austin, A. J.; Cammi, R.; Pomelli, C.; Ochterski, J. W.; Ayala, P. Y.; Morokuma, K.; Voth, G. A.; Salvador, P.; Dannenberg, J. J.; Zakrzewski, V. G.; Dapprich, S.; Daniels, A. D.; Strain, M. C.; Farkas, O.; Malick, D. K.; Rabuck, A. D.; Raghavachari, K.; Foresman, J. B.; Ortiz, J. V.; Cui, Q.; Baboul, A. G.; Clifford, S.; Cioslowski, J.; Stefanov, B. B.; Liu, G.; Liashenko, A.; Piskorz, P.; Komaromi, I.; Martin, R. L.; Fox, D. J.; Keith, T.; Al-Laham, M. A.; Peng, C. Y.; Nanayakkara, A.; Challacombe, M.; Gill, P. M. W.; Johnson, B.; Chen, W.; Wong, M. W.; Gonzalez, C.; Pople, J. A. *Gaussian 03*, B.04; Gaussian, Inc.: Wallingford, CT, 2004.
- (19) Cramer, C. J. *Essentials of Computational Chemistry*; Wiley: Chichester, 2004.

JP902150V